



# CFD Analysis on Solar Photovoltaic Thermal Collector System with Various Tube Geometry

Sippu Kumar<sup>1</sup>, Dr. S.S. Pawar<sup>2</sup>

<sup>1</sup>Research Scholar, Department of Mechanical Engineering, Sarvepalli Radhakrishnan University, Bhopal

<sup>2</sup>Registrar, Department of Mechanical Engineering, Sarvepalli Radhakrishnan University, Bhopal

OPEN ACCESS

Volume: 5

Issue: 2

Month: May

Year: 2026

ISSN: 2583-7117

Published: 19.05.2026

Citation:

Sippu Kumar, Dr. S.S. Pawar “CFD Analysis on Solar Photovoltaic Thermal Collector System with Various Tube Geometry” International Journal of Innovations in Science Engineering and Management, vol. 5, no. 2, 2026, pp. 216-229.

DOI:

10.69968/ijisem.2026v5i2216-229



This work is licensed under a Creative Commons Attribution-Share Alike 4.0 International License

## Abstract

The present study aims to reduce excessive temperature in photovoltaic (PV) modules by optimizing the cooling tube geometry in a photovoltaic–thermal (PV/T) collector. CATIA V5 was used to create a three-dimensional steady-state thermal model. A glass cover, a PV layer positioned between EVA layers, a Tedlar back sheet, an absorber plate, a cooling tube, and insulation are all part of the computational domain. Three tube geometries—U-tube, 3-pass tube, and rectangular wave-shaped tube—were analyzed for heat transfer performance. ANSYS Fluent was used to model the thermo-fluid behaviour using the SIMPLE algorithm for pressure-velocity coupling and the finite volume approach. With a mass flow rate of 0.012 m/s and an input temperature of 30 °C, water was used as the working fluid under 1000 W/m<sup>2</sup> of solar radiation. Results show that tube geometry significantly influences temperature distribution and heat transfer. Among the configurations, the 3-pass tube (Case 2) achieved the lowest PV temperature and an outlet water temperature of 51.06 °C with a heat transfer rate of 1057.11 W, indicating improved thermal management and collector performance.

**Keywords;** PV/T Collector, Tube Geometry Optimization, Thermal Management, Heat Transfer Analysis, CFD Simulation.

## INTRODUCTION

The growing rate of energy demands in the world, the exhausting nature of fossil fuel resources, and the mounting environmental concerns have necessitated an urgent need to come up with sustainable and renewable energy systems. Traditional sources of energy like coal, petroleum, and natural gas are not only scarce but also cause a lot of pollution and climatic change to the environment due to emission of greenhouse gases [1]. Researchers and policymakers worldwide are being compelled to investigate renewable energy sources that are pure, sustainable, and environmentally favourable. Out of the other renewable energy sources, solar energy has been introduced as one of the richest and promising sources of energy due to its free availability, inexhaustible, and not concentrated in limited locations among the world [2]. Various technologies can be used to convert solar radiation into solar energy with solar photovoltaic (PV) systems being the most common in converting solar energy into electrical energy. Nevertheless, traditional photovoltaic panels can usually only change a small fraction of the incident sun radiation into electricity, with the rest being wasted as heat [3], [4]. This surplus heat warms the PV cells thus decreasing their electrical efficiency and performance. In a bid to eliminate this limitation and harness the wasted thermal energy, solar photovoltaic thermal (PVT) collectors have been invented [5], [6].

An integral system that simultaneously produces thermal energy and electrical energy from the same solar radiation is known as a solar photovoltaic thermal collector. In this system, a thermal collector is attached to the backside of the photovoltaic panel, allowing a working fluid such as water or air to flow through the collector and remove excess heat from the PV module [7]. While the extracted heat may be utilised for a variety of thermal purposes, including drying, industrial operations, water heating, and space heating, this process aids in cooling the solar cells, increasing their electrical efficiency [8], [9].

The importance of solar PVT collectors lies in their ability to utilize solar energy more efficiently compared to conventional PV or solar thermal systems operating separately. By integrating thermal and electrical energy generation into a single device, PVT collectors optimise the utilisation of solar radiation and increase the overall energy output [10], [11]. Additionally, these technologies promote sustainable energy development, reduce dependency on fossil fuels, and reduce greenhouse gas emissions. Therefore, solar photovoltaic thermal collectors are considered a promising technology for meeting future energy demands while supporting the transition toward clean and renewable energy systems [12], [13].

**Principle of Solar Energy: The Photovoltaic Effect**

The photovoltaic (PV) effect is the process of turning solar energy into electrical power. In a PV system, the PV

cells exert this action. The P-N structure is the internal electric field produced by doping the semi-conducting components of the PV cell. P-type (positive) silicon often loses electrons and gains holes, whereas n-type (negative) silicon absorbs electrons [14], [15]. When sunlight hits a semiconductor cell, photons in the light excite some of the electrons, forming electron-hole (negative-positive) pairs. Due to the internal electric field, these pairings are subjected to separation. As a result, the electrons travel to the negative electrode and the holes to the positive electrode. A conducting wire connects the negative electrode, load, and positive electrode in series to form a circuit. As a result, an electric current supplies the external load. This is how the PV effect of a solar cell works [2], [16].

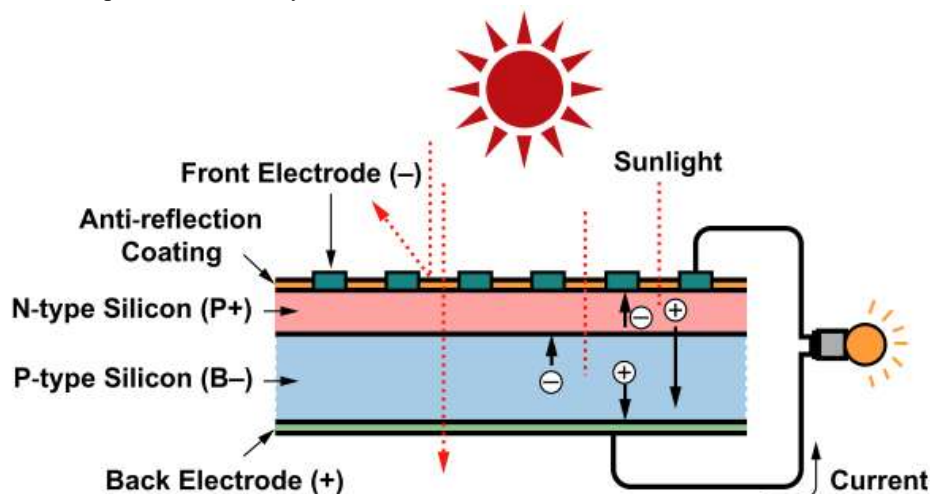
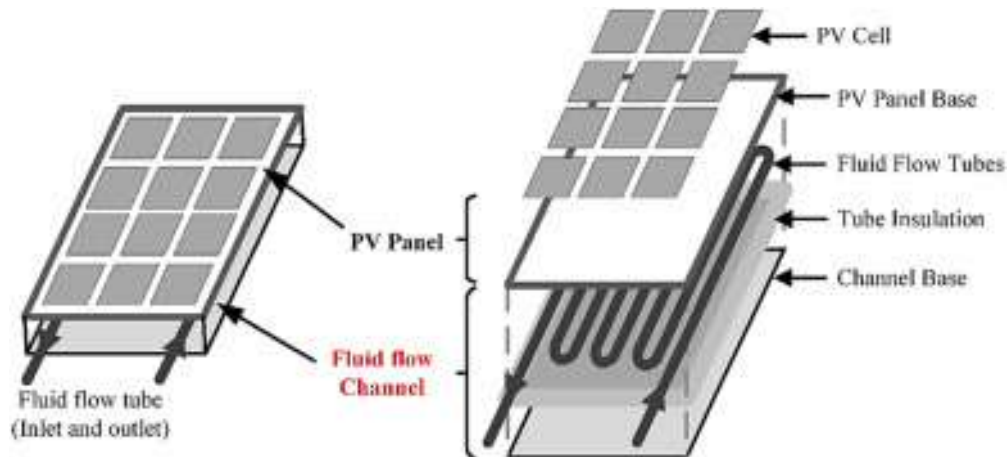


Figure 1: Photovoltaic effect in a solar cell [7]

The similar process happens when light hits a silicon crystal. If the input light intensity is strong enough, the crystal will absorb enough photons, which will then activate part of the covalent bond's electrons. These excited electrons then acquire sufficient energy to transition from the valence band to the conduction band [17]. The electrons depart the covalent link due to their energy level being in the conduction band, resulting in a cavity in the bond that is eliminated. These are termed free electrons travel arbitrarily inside the crystal structure of the silicon. In a solar cell, these free electrons and holes are essential for producing energy. Consequently, these holes and electrons are called light-generated holes and electrons, respectively. The silicon crystal cannot create electricity on its own from these light-generated electrons and holes [18].

**Solar Photovoltaic Thermal Collectors**

Photovoltaic thermal collectors, also referred to as "hybrid solar collectors, photovoltaic thermal solar collectors, PV/T collectors, or solar cogeneration systems", are solar power generation technologies that convert solar radiation into consumable thermal and electrical energy [19]. They are typically abbreviated as PVT collectors. While photovoltaic solar cells convert sunlight into electricity, a solar thermal collector is employed to transfer the unused excess heat from the PV module to a heat transfer fluid [20]. PVT collectors are a combination of these two technologies. By combining electricity and heat generation into a single component, these technologies can reach a better overall effectiveness than "solar photovoltaic (PV) or solar thermal (T) alone" [21].



**Figure 2: Schematic of hybrid PV/T collector, PV panel integrated with thermal cooling system using nano-fluid** [12]

This system's main characteristic is that a PV panel's efficiency drops as cell temperature rises. Heat from the PV cells is removed by water or air passing through the thermal collector, enabling more effective operation. Additionally, power and water or air heating may be generated in the same footprint, making better use of precious roof space. PV-T technologies come in a variety of forms. The intended uses, installed costs, and performance attributes of each technology vary [2]. As the temperature rises, solar photovoltaic cells lose efficiency, which can be significant on hot, bright days. Additionally, some energy is "lost" to the environment due to solar PV's inefficiency. Solar PV need a partner who can balance out its weaknesses and enhance its strengths [22].

A solar thermal collector can be positioned behind a solar photovoltaic (PV) array to cool the PV cells. Simultaneously, the solar collector is able to recover for productive use the majority of the energy that would otherwise be wasted as it travels through the array [9]. The gathered energy is transferred by the collector to a circulating media, such as fluid or air, which subsequently carries it to a place where it can be used or stored, such as a building, a hot water tank, or the ground, for later recovery by a heat pump. In the optimum scenario, the solar PV cells are chilled to a more suitable operating temperature, preferably around 25°C, when they come into contact with the solar thermal collector. By providing both heat and electrical energy, the union creates a solar co-generation process [23]. The idea is rational and appealingly straightforward. However, it has taken some time for the coin to drop in an industry that is deeply rooted in the

technology of individual gadgets. When it occurs, it may be a revelation [24].

To cool the system—that is, to move the heat energy away from the PV module—air, water, and air-water hybrid systems have been employed. Although PVT-air systems are more advanced, PVT-water systems have lately shown signs of fast growth [8]. The focus on water systems and their quick development may be explained by the fact that water has a larger specific heat capacity than air, as well as a greater requirement for and use of hot water. PV cells and solar thermal collectors can be combined in a variety of ways [16]. There are several commercial PVT collectors that fall into the following groups based on their heat transfer fluid and fundamental design:

**PVT liquid collector:** The PV cell must be cooled and its temperature lowered in order for the PV/T system to produce more heat and power. This is a difficult endeavour, particularly in regions with hot, humid climates. An efficient cooling method for PV/T panels is lacking. Compared to air-based systems, “liquid-based photovoltaic thermal collectors” are much more effective and desirable. Compared to “air-based PV/T collectors”, which are sensitive to variations in solar radiation levels, liquid-based PV/T collectors have far less temperature fluctuation. In liquid-based PV/T collectors, the most common working fluids are "water, water/air, and, more recently, refrigerant". PVT collectors of the water type are the most extensively researched system [22].

**PVT air collector:** Compared to PVT liquid collectors, which require thermal collecting materials coupled to traditional PV modules, PVT air collectors have a significant

benefit. Nevertheless, the air type necessitates a substantial volume of air flow to achieve an acceptable level of thermal efficiency, which presents challenges in the form of pollution, fan losses, and large diameter conduit concerns. Problems might arise from the enormous tubing needed, particularly when retrofitting. Compared to water, using air as a heat-transfer medium offers certain benefits but also significant drawbacks. Benefits include the absence of freezing, boiling of the accumulating fluid, and any potential damage in the event of a spill. The drawbacks, however, are rather serious: low heat conductivity and low heat capacity lead to low density and low heat transfer, necessitating large volume transfer. In light of this, a PVT air collector's performance evaluation is crucial for its use in buildings

[10]. The performance of a PVT air collector depends on a number of climatic, operational, and design factors, including the "air collector's length and width, solar radiation intensity, wind speed, solar cell temperature, back surface temperature, inlet and outlet air, and inlet air velocity". The PVT air collector's collected air may be used as the building's heat source. Pre-heated fresh air may be fed into the building's ventilation system using the hot air from the PVT collector. Improving indoor air quality (IAQ) requires breathing in fresh, outside air, yet doing so raises the building's ventilation energy demand. In order to increase the IAQ and thermal efficiency of buildings with heat recovery, a Heat Recovery Ventilation (HRV) system has been implemented [21].

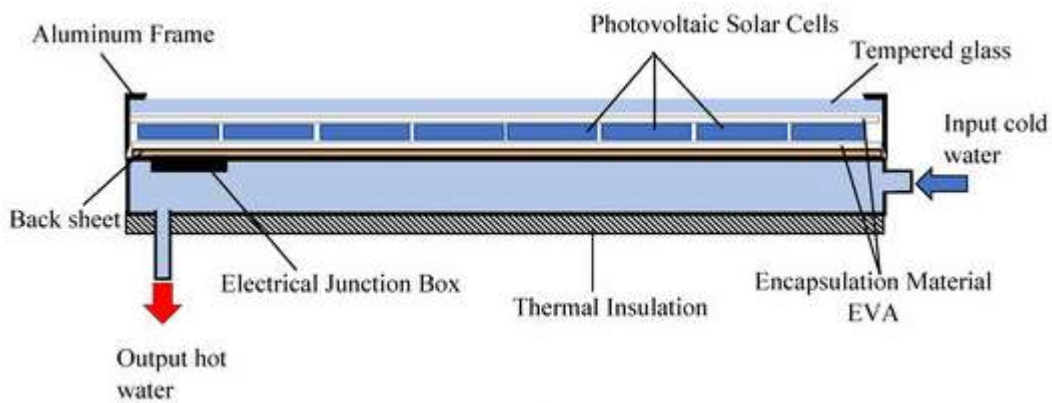


Figure 3: Schematic diagram of PVT water (liquid) collector [8]

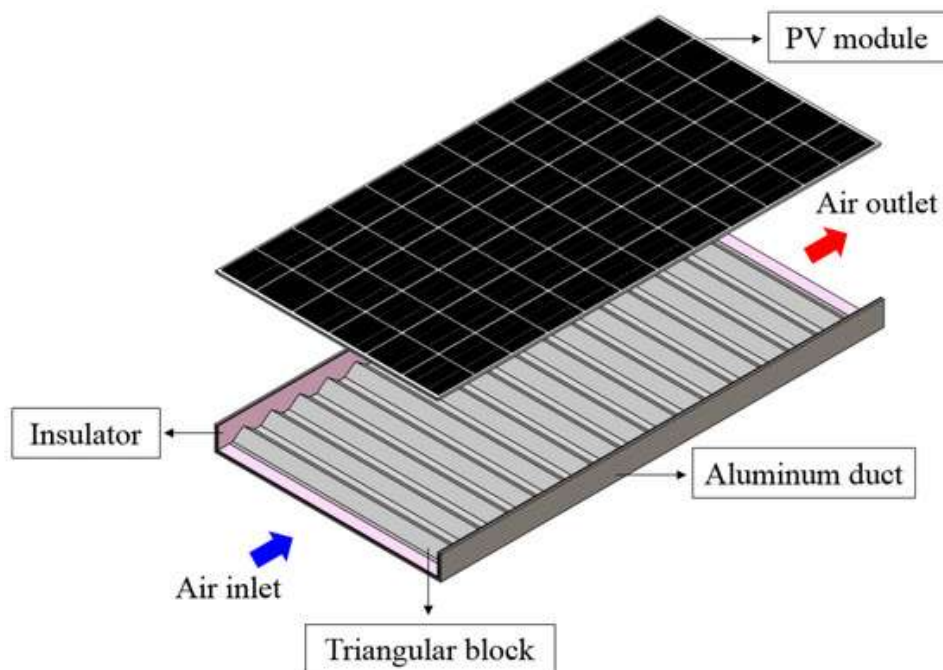


Figure 4: Systematic diagram of PVT air collector [10]

### Effect of Temperature on Different Photovoltaic Technologies

Photovoltaic module manufacturers usually only offer ratings under one operating condition, such as STC. On the other hand, PV modules function in a wide variety of field situations. Therefore, the information provided by the manufacturer is insufficient to ascertain the module's real performance in the field. The appropriateness of PV module technology for a particular location is determined by five critical factors: "the annual solar intensity distribution, the efficiency of PV module technology as a function of intensity, the annual temperature distribution and module temperature coefficient, the solar spectrum distribution, and the rate of power degradation of PV modules over time" [18]. The ambient temperature affects the solar module's electrical efficiency, which decreases as the temperature rises. The majority of semiconductor material properties are affected by temperature increases because they narrow a semiconductor's band gap. The energy of the electrons in a semiconductor can be conceived of as increasing as the temperature increases, resulting in a decreasing band gap [22]. The measure primarily affected by an increase in temperature is the open circuit voltage. The temperature coefficient shows how much the power output will decrease if the temperature of the PV module deviates from STC. It is also true that different solar cell technologies have different temperature coefficients [25].

### RESEARCH METHODOLOGY

#### System Configuration

A photovoltaic module at the top of the solar photovoltaic-thermal collector converts incident solar energy into electrical energy, while a solar thermal collector at the bottom recovers heat energy from the photovoltaic module. The total system output is increased by this extraction of thermal and electrical energy. To collect thermal energy, the solar module's bottom is equipped with an absorber plate and cooling tubes.

In addition to providing electrical insulation and stability, "the solar photovoltaic-thermal collector system configuration" is illustrated in Figure 4. The photovoltaic layer is protected from moisture and grime by layers of EVA, Tedlar, and glass. The glass cover utilised has a high transmissivity to solar insolation due to its low iron content. The EVA layer acts as a cushion and electrical insulator to shield the solar cell from any mechanical harm brought on by elevated pressures. The polyvinyl fluoride Tedlar, also known as the back-sheet, gives the solar cell strength and mechanical stability. The thermal absorber, a conventional flat plate collector, is created by welding cooling tubes with a circular cross section onto the back of the absorber plate. The aluminium absorber panel is connected to the cooling tubes, which are composed of copper, a material with a high heat conductivity.

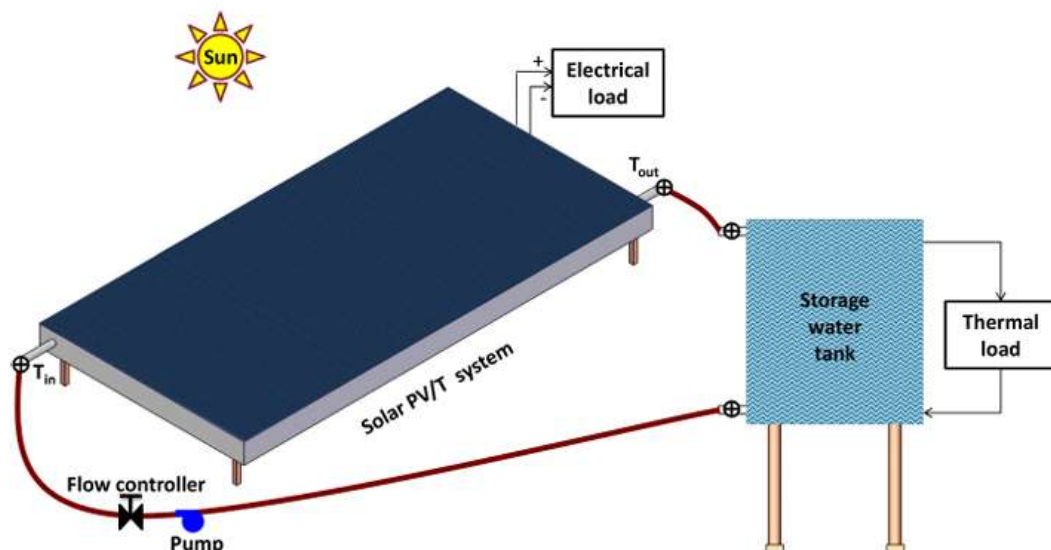


Figure 5: Schematic of the solar PV-T collector system

The model is designed to enhance the efficacy of a 380W<sub>pe</sub> panel, which is configured in a 12 × 6 array containing the cells. The arrangement of the cooling tubes

allows two riser tubes to cool each row of solar cells underneath it. Thermal bonding between the cooling tubes and the absorber plate improves heat transmission even

further. Rock wool is used to insulate the collector's bottom, and an aluminium frame encloses the whole collector unit. In order to cool the solar module and extract thermal energy, water is subsequently circulated through the cooling tunnels. This guarantees that there are no hotspots or thermal stress buildup while the panel runs within acceptable temperature limits.

### Computational Configuration

Using CATIA V5, a three-dimensional steady state thermal model was created. The temperature distribution of the photovoltaic-thermal collector over different layers is obtained by simulation. The system unit that corresponds to a single cooling tube is selected for modelling in order to minimise the computational cost. This is because, in the low-rate range of the current investigation, the minimal pressure drops associated with single-phase flow are expected to

provide a uniform flow distribution throughout all the riser tubes.

In the computational domain, there is a photovoltaic semiconductor material layer with a protective and insulating glass cover, a photovoltaic layer inserted "between two EVA layers, a Tedlar/back sheet, an absorber plate, a cooling tubing, and insulation". The dimensions of the computational model are 120 mm in width and 1560 mm in length. The computational domain is depicted in Fig. 5. Table 1 lists the thermo-physical characteristics of a photovoltaic-thermal collector's different layers. CATIA V5 was used to create the three-dimensional geometry. The computational domain is then created by meshing the geometric model with unstructured hexahedral and tetrahedral pieces. A proper inflation of seven layers from the wall in the fluid domain was given in order to photograph the boundary layer phenomena.

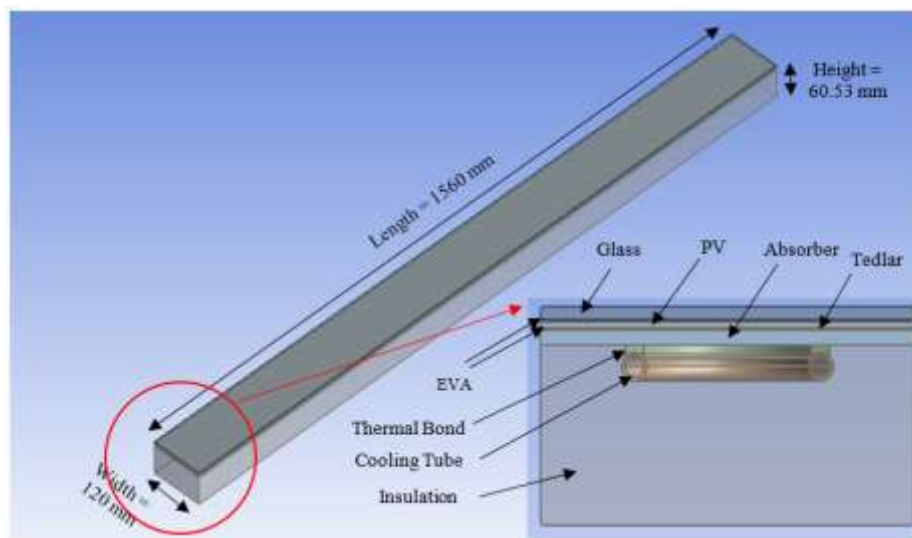


**Figure 6: Computational domain of solar photovoltaic thermal collector system**

The figure 6-8 illustrates three different tube geometries used for heat transfer analysis, namely the U-tube configuration, 3-pass tube configuration, and rectangular wave-shaped tube configuration. In the first configuration, the U-tube geometry consists of a straight tube of total length approximately 1500 mm, which bends smoothly at one end forming a U-shaped return path. The tube spacing between the two parallel sections is about 60 mm. This arrangement allows the fluid to enter from one end, travel along the straight section, and then return through the adjacent parallel section after the bend. The side and front views show that the tube maintains a uniform cross-section along its entire length, ensuring consistent flow characteristics. In the

second configuration, the 3-pass tube design increases the flow path length by introducing an additional return bend. The overall tube length remains about 1500 mm, while the effective straight section before the bend is approximately 1440 mm. The spacing between the parallel tube sections is around 40 mm. This configuration allows the working fluid to pass through three consecutive segments of the tube, enhancing heat transfer by increasing the residence time and surface contact area. The third configuration represents a rectangular wave-shaped tube, where the tube follows a periodic zigzag pattern instead of smooth bends. The total length of this configuration is approximately 1560 mm with a wave amplitude spacing of about 80 mm. The repeated

rectangular bends create multiple flow disturbances and secondary vortices, which promote better mixing of the fluid and improve the heat transfer performance compared with

conventional straight or U-shaped tubes. In this study there are 3 cases considered mention in table 2.

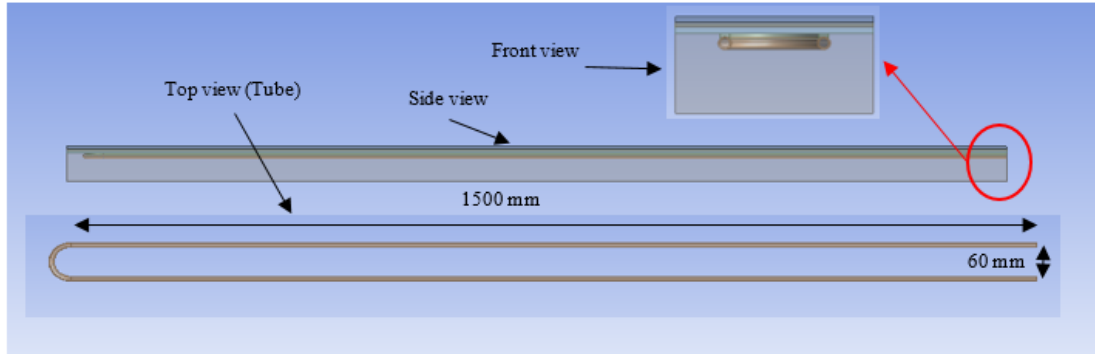


**Figure 7: U-tube configuration**

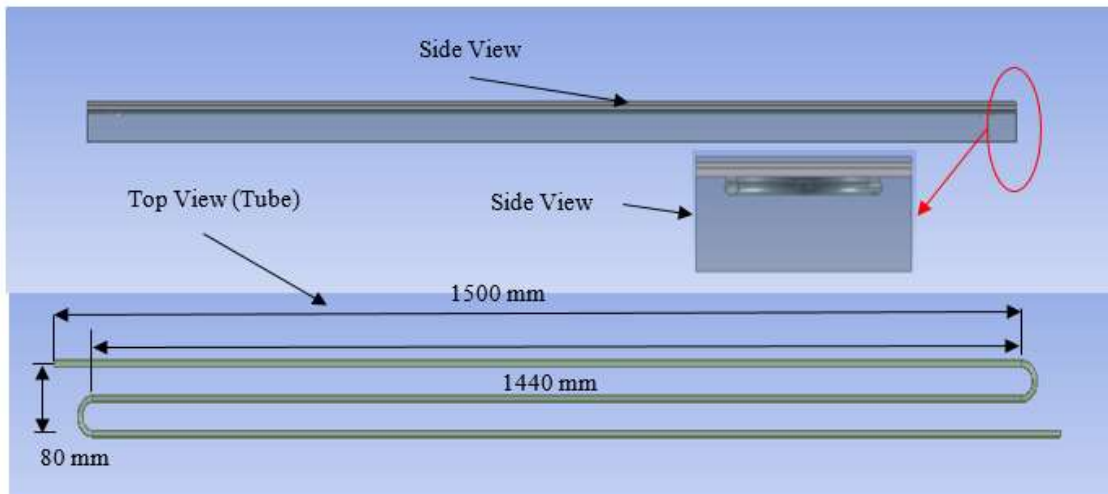


**Figure 8: 3-Pass tube configuration**

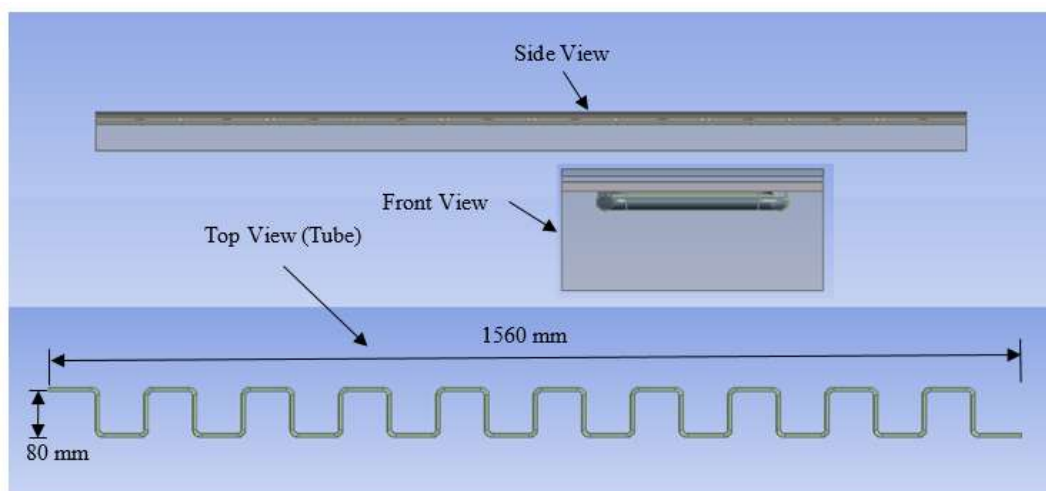


**Figure 9: Rectangular wave-shaped tube configuration**

**Table 1: Thermo-physical Properties of various layers of PV-Y collector**

| Layer                      | Thickness (mm) | Thermal conductivity (W/m K) | Density (kg/m <sup>3</sup> ) | Specific heat capacity (J/kg K) |
|----------------------------|----------------|------------------------------|------------------------------|---------------------------------|
| Glass cover                | 3.2            | 1                            | 3000                         | 500                             |
| EVA top layer              | 0.5            | 0.4                          | 960                          | 2090                            |
| PV                         | 2              | 148                          | 2330                         | 677                             |
| EVA bottom layer           | 0.5            | 0.4                          | 960                          | 2090                            |
| Tedlar                     | 0.33           | 0.4                          | 1200                         | 1250                            |
| Absorber plate (Aluminium) | 4              | 204                          | 2710                         | 910                             |
| Cooling tube (copper)      | 1              | 386                          | 8940                         | 390                             |
| Insulation                 | 50             | 0.05                         | 180                          | 1515                            |
| Water                      | -              | 0.63                         | 998.2                        | 4183                            |

**Table 2: Cases overview**

| Cases  | Computational configuration                |
|--------|--------------------------------------------|
| Case 1 | U-tube configuration                       |
| Case 2 | 3-Pass tube configuration                  |
| Case 3 | Rectangular wave-shaped tube configuration |

**Mesh Generation**

To facilitate the numerical solution of the governing equations and discretise the geometry of "the solar photovoltaic-thermal (PV/T) collector", the computational domain was meshed in ANSYS Fluent. In order to precisely represent the heat transfer and fluid flow behaviour within the collector system, the mesh creation procedure splits the whole computational domain into a large number of tiny finite elements. In an effort to attune computational accuracy and efficiency, the present investigation implemented two distinct element sizes. A relatively coarse mesh with an

element size of 5 mm was applied to the insulation region, as the thermal gradients in this area are comparatively lower. In contrast, a finer mesh with an element size of 0.8 mm was applied to the remaining regions of the collector, including the tube and absorber sections, to accurately resolve the fluid flow and temperature distribution. The mesh consisted of a combination of tetrahedral and hexahedral elements, which helps in effectively representing the complex geometry of the tube configurations. The total number of elements generated during the meshing process for the U-type tube, 3-pass tube, and rectangular wave-shaped tube configurations were 7,293,058, 8,332,446, and 7,218,106, respectively. Correspondingly, the number of nodes produced for these configurations were 7,654,886, 8,292,562, and 7,577,193. This high-density mesh ensures improved numerical accuracy in predicting the thermal and flow characteristics of the PV/T collector. The meshed computational domains for the different tube configurations are illustrated in Figure 9, which presents the detailed mesh structure used for the numerical simulations.

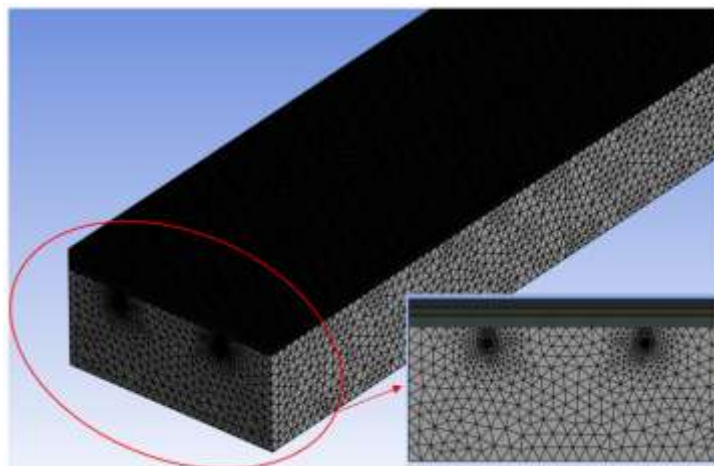


**Figure 10: Meshing of computational domain of solar photovoltaic thermal collector**

### Governing Equations

This section delves into the mathematical models and governing equations that are employed to simulate “the photovoltaic-thermal collector”. The body force due to gravitation is zero in the x and z directions, and  $(-gy)$  in the y direction, as the panel is expected to be at a zero inclination. For a steady-state, single-phase flow, the equations for mass conservation (Eq. (1)), momentum conservation (Eq. (2)), and energy conservation (Eq. (3)) are as follows:

$$\nabla \cdot (\rho \vec{u}) = 0 \quad \text{eq. (1)}$$

$$\rho(u \cdot \nabla)u = -\nabla P + \rho \vec{g} + \mu \nabla^2 \vec{u} \quad \text{eq. (2)}$$

$$P(\nabla \cdot \vec{u}) = \nabla \cdot (k \nabla T) + (\rho \dot{q}) \quad \text{eq. (3)}$$

The discrete ordinate (DO) radiation model is used to simulate the radiation heat transfer from the glass cover to the sky. The uncoupled technique, which solves the radiation intensity and energy equations sequentially, is used to construct the DO model.

$$\frac{\partial I}{\partial x_i} + (a + \sigma_s)I(r, s) = an^2 \frac{\sigma T^4}{\pi} + \frac{\sigma_s}{4\pi} \int_0^{4\pi} I(r, s') \varphi(s, s') d\Omega' \quad \text{eq. (4)}$$

### Numerical Procedure

The thermo-fluid problems were resolved using the ANSYS FLUENT finite volume method with the k-omega viscous model. After discretisation and suitable linearisation, “the non-linear partial differential equations” are reduced to algebraic equations. The second-order upwind approach is used to discretise pressure, momentum, and energy, and “the least squares cell-based algorithm” is used to assess the gradients. Pressure and velocity connections are established through the SIMPLE method, which involves the substitution of an initial pressure field into the momentum equation to produce the velocity field. The estimated pressure field is kept if the computed velocity field satisfies the continuity equation; if not, a pressure correction factor is applied until the velocity field does. The model's governing equations are all linked and non-linear. Consequently, the convergence criteria are satisfied by solving these equations simultaneously until the residuals for all equations are less than  $1 \times 10^{-6}$ .

### Boundary Conditions

The computational domain's boundaries must be defined with suitable boundary conditions in order to solve the governing equations. Both thermal and flow boundary conditions are provided since “the three-dimensional model of the photovoltaic/thermal (PV/T) collector” comprises simultaneous heat transfer and fluid flow operations. Since the collector operates in an open atmospheric environment, the model represents the physical conditions present in the surrounding ambient atmosphere. Only a small portion of the incident solar energy is converted into electrical energy in a photovoltaic system, while the remaining portion is dissipated as heat within the system. Since the collector's exterior surfaces are subject to both radiative and convective heat transfer, these multiphysics interactions must be represented by a mixed boundary condition. Convection is solely taken into account at the collector's upper and bottom

surfaces for simplicity. Consequently, the top surface of the glass cover and the bottom surface of the rear insulating layer are respectively assigned a wind convection heat transfer coefficient and a free-stream temperature that is equivalent to the ambient temperature. Additionally, the PV/T collector radiates heat to the sky based on the temperature difference between the collector surface and the sky. The emissivity of the radiating surfaces and the sky temperature are specified to simulate the radiative heat exchange between the glass cover and the sky. By adding a velocity boundary condition at the intake and a pressure outlet condition at the exit, the fluid flow inside the tube is modelled. The working fluid is water, which has an “inlet temperature of 30 °C and an inlet mass flow rate of 0.012 m/s”. Additionally, it is assumed that the solar irradiation incident on the photovoltaic surface is 1000 W/m<sup>2</sup>.

### Numerical and Computational Validation

For further analysis of the solar photovoltaic–thermal (PV/T) collector, it is essential to first validate the computational domain, numerical approach, and applied boundary conditions. The PV/T collector model used in this study is made up of many protective layers, such as EVA, Tedlar, and a glass cover, which shield the solar module from moisture and dust while also giving it structural stability and electrical insulation. The computational model has a total length of 1560 mm and a width of 120 mm. By conducting a comparison between the simulation results and the experimental data reported by Parthiban (2020) [26], the numerical model that has been developed is verified. For validation purposes, the outlet temperature of water is considered as the primary parameter.

Circular cooling tubes are welded to the rear side of the absorber plate of “the PV/T collector's thermal absorber”, which is constructed from a conventional flat plate collector arrangement. The copper cylinders, which possess a high

thermal conductivity, are fixed to an aluminium absorber plate in order to enhance heat transfer. In this validation model, a straight tube configuration is considered. Water is the working fluid that travels through the tube, which has a wall thickness of 1 mm and an inner diameter of 6 mm. ANSYS Fluent, which solves thermo-fluid governing equations using the finite volume approach, is used for the numerical simulation. The pressure-velocity coupling is generated using the SIMPLE method. The velocity field is obtained by substituting an initial pressure field into the momentum equations. If the calculated velocity field satisfies the continuity equation, the assumed pressure field

is maintained; otherwise, pressure corrections are applied periodically until convergence is achieved.

The inlet mass flow rate of water as it enters the conduit is 0.012 m/s, and “the inlet temperature is 30 °C”. On the photovoltaic surface, the incident solar irradiance is 1000 W/m<sup>2</sup>. The comparison between the present simulation and the results reported by Parthiban (2020) [26] shows a very small deviation of 0.58 °C in the outlet water temperature, indicating good agreement and confirming the accuracy of the developed model. The validation results of the outlet water temperature are illustrated in Figure 10.

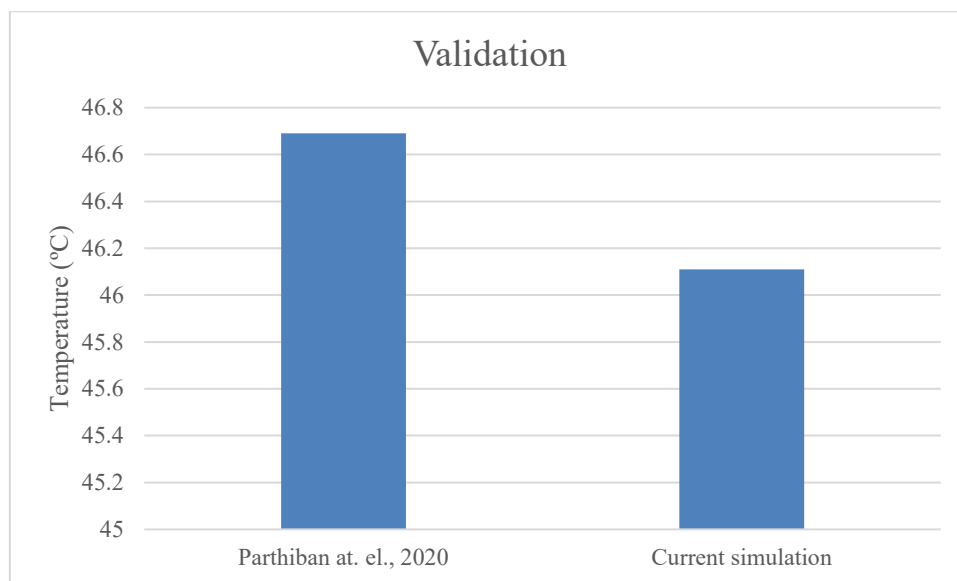


**Figure 11: Validation result of Solar PV-T collector**

## RESULT AND DISCUSSION

### *Temperature Distribution*

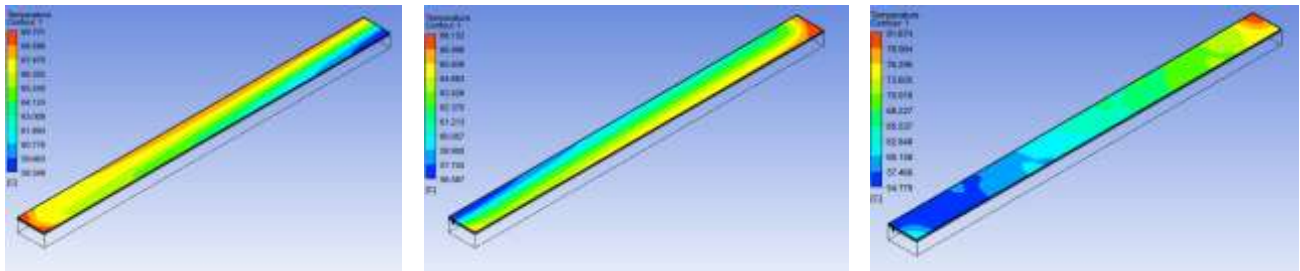
By analysing the temperature contours of the PV layer, absorber plate, and cooling tube, as well as the outflow temperature of water, "the temperature distribution within the photovoltaic–thermal (PV/T) collector" was analysed for three distinct cases. In Case 1, the temperature of the photovoltaic layer ranges from 58.54 °C to 69.7 °C, with an average temperature of 65.476 °C, as illustrated in Figure 11. The absorber plate shows a temperature range of 41.117 °C to 58.135 °C with an average value of 51.624 °C, while the tube temperature varies between 36.74 °C and 53.39 °C, giving an average temperature of 48.04 °C. The outlet temperature of water for this case is 51.086 °C. The reason for the PV layer's comparatively greater temperature is that it receives solar radiation directly and only partially transforms it into electrical energy; the remaining energy is transformed into heat and sent to the absorber and tube.

In Case 2, the PV temperature slightly decreases and varies from 56.587 °C to 68.152 °C, with an average value of 62.618 °C. The absorber plate temperature ranges from 39.368 °C to 55.785 °C with an average temperature of 48.756 °C, and the tube temperature varies between 35.614 °C and 54.141 °C, with an average of 46.686 °C. The outlet water temperature is 51.06 °C. The reduction in average temperatures in this case indicates improved heat removal by the cooling tube, which enhances the heat transfer from the PV layer to the circulating water.

In Case 3, the PV temperature ranges from 54.779 °C to 81.674 °C, with an average temperature of 64.026 °C, while the absorber plate temperature varies between 38.401 °C and 71.056 °C, having an average value of 50.162 °C. The tube temperature ranges from 35.016 °C to 57.564 °C, with an average of 45.453 °C, and the outlet water temperature reaches 51.094 °C. The wider temperature range in this case is mainly due to the geometric variation in the tube

configuration, which creates non-uniform heat transfer regions and localized thermal accumulation. Overall, the slight differences in outlet water temperature among the three cases indicate that tube configuration influences the

internal heat transfer distribution within the collector, while the outlet temperature remains relatively stable due to the constant inlet conditions and mass flow rate of the working fluid.

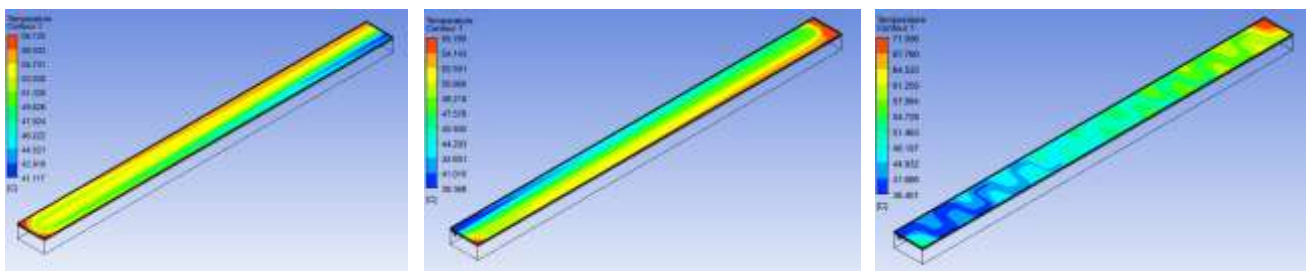


Case 1 (u-tube configuration)

Case 2 (3-pass tube configuration)

Case 3 (Rectangular wave-shape tube configuration)

**Figure 12: Temperature distribution in PV at all cases**

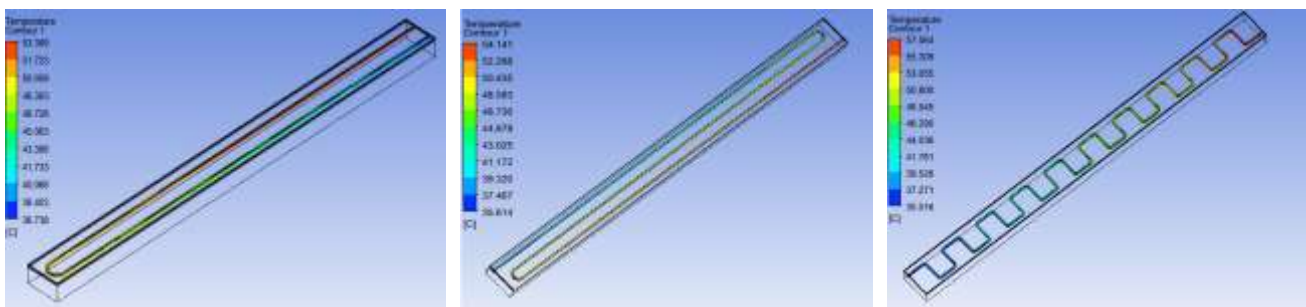


Case 1 (u-tube configuration)

Case 2 (3-pass tube configuration)

Case 3 (Rectangular wave-shape tube configuration)

**Figure 13: Temperature distribution in absorber at all cases**



Case 1 (u-tube configuration)

Case 2 (3-pass tube configuration)

Case 3 (Rectangular wave-shape tube configuration)

**Figure 14: Temperature distribution in tube at all cases**

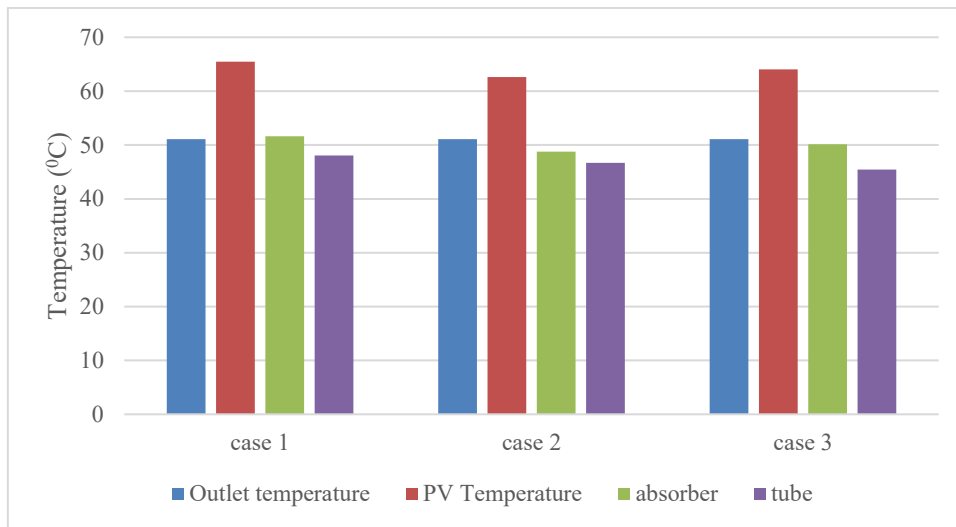


**Figure 15: Temperature in PV, absorber, tube, and Outlet temperature in all cases**

**Heat Transfer Rate**

The heat transfer rate obtained for the three different tube configurations shows only a slight variation among the cases. In Case 1, the heat transfer rate is 1058.43 W, while in Case 2 it is 1057.11 W, and in Case 3 it reaches 1058.84 W. The graphical comparison of these values is presented in Figure 15. The small differences in the heat transfer rate are mainly attributed to the variation in tube geometry used in each configuration. In Case 1, the tube arrangement provides a relatively uniform flow path, which allows effective heat transfer between the absorber plate and the circulating water. In the second case, the slight decrease in heat transfer rate may be attributed to the modification in tube configuration, which alters the fluid flow pattern. This change results in minor variations in the local velocity distribution and the development of a thermal boundary layer along the tube

wall. The efficiency of heat transport may be somewhat decreased by these modifications. In Case 3, the heat transfer rate is marginally higher compared with the other cases because the modified tube geometry increases the effective contact length between the absorber plate and the fluid flow path. The presence of bends or variations in the tube shape can promote additional fluid mixing and small-scale turbulence, which enhances the convective heat transfer coefficient. However, since the inlet conditions, solar irradiance, and material properties remain constant in all cases, the overall heat transfer rates are very close to each other. Therefore, the variation in tube geometry mainly influences the internal flow characteristics and local heat transfer behavior, leading to only minor differences in the total heat transfer rate of the solar PV/T collector system.

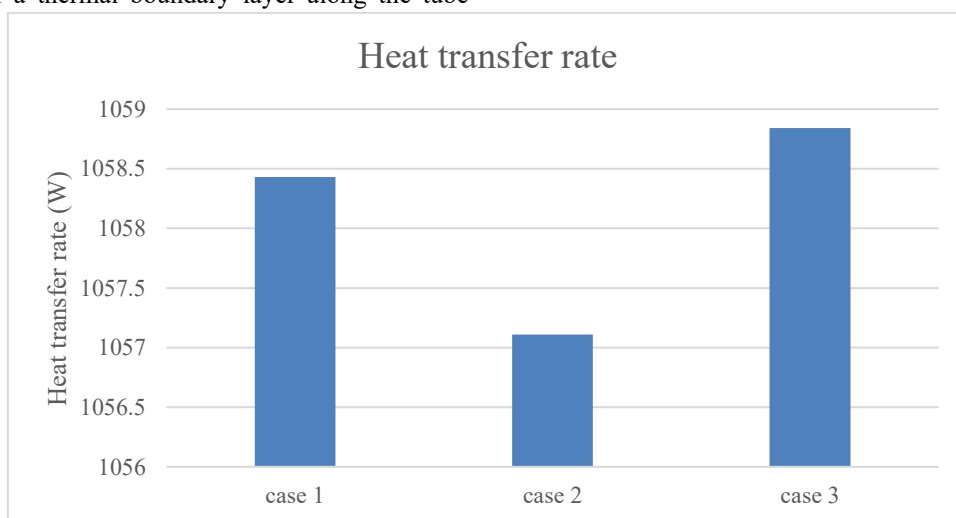


**Figure 16: Heat transfer rate of all cases**

## CONCLUSION

The thermal efficacy of a solar photovoltaic–thermal (PV/T) collector with three distinct tube configurations was investigated in the current study by analysing "the temperature distribution in the photovoltaic layer, absorber plate, cooling tube, water discharge temperature, and overall heat transfer rate". The findings show that tube shape significantly affects the collector's internal heat transfer behaviour and temperature distribution. In all cases, the PV layer recorded the highest temperature since it directly receives solar radiation, while the absorber plate and cooling tube exhibited comparatively lower temperatures due to the continuous removal of heat by the circulating water. Regardless of the tube configuration, the working fluid efficiently absorbed the available thermal energy, as seen by the nearly constant outlet water temperature in all three scenarios. Similarly, the total heat transfer rate was also very close in all cases, showing that the collector performance remained nearly constant under the same operating conditions. However, a slight variation in temperature distribution was observed due to the differences in tube geometry, which influence the flow path, fluid mixing, and heat transfer characteristics. Among the three configurations, Case 2 showed the lowest average temperature in the PV layer, which is desirable because reducing the PV temperature improves the electrical efficiency and prevents overheating of the photovoltaic cells. Therefore, Case 2 is considered the most effective configuration for the PV/T collector system.

- Average PV temperature is 62.618 °C, which is lower than the other cases, indicating improved cooling of the photovoltaic layer.
- The temperature in the PV layer varies between 56.587 °C and 68.152 °C, showing a relatively uniform thermal distribution.
- The absorber plate records an average temperature of 48.756 °C, with a temperature range of 39.368 °C to 55.785 °C, indicating efficient heat transfer from the PV layer to the absorber.
- The cooling tube exhibits an average temperature of 46.686 °C, with temperatures ranging from 35.614 °C to 54.141 °C, confirming effective heat absorption by the circulating water.
- The outlet temperature of water is 51.06 °C, demonstrating that the working fluid effectively removes heat from the collector.
- The overall heat transfer rate is 1057.11 W, which is comparable to the other cases while maintaining the lowest PV temperature.

These results indicate that Case 2 provides better thermal management of the PV layer while maintaining effective heat transfer performance in the solar PV/T collector.

## REFERENCES

- [1] O. Richard, A. Turala, V. Aimez, M. Darnon, and A. Jaouad, "Low-Cost Passivated Al Front Contacts for III-V/Ge Multijunction Solar Cells," *Energies*, vol. 16, 2023.
- [2] R. A. M. Lameirinhas, J. P. N. Torres, and J. P. de M. Cunha, "A Photovoltaic Technology Review: History, Fundamentals and Applications," *Energies*, vol. 15, 2022.
- [3] H. Nazir *et al.*, "Recent developments in phase change materials for energy storage applications: A review," *Int. J. Heat Mass Transf.*, vol. 129, 2019, doi: 10.1016/j.ijheatmasstransfer.2018.09.126.
- [4] S. K. Shah, B. K. Arjariya, and P. Bhawsar, "Design Formulation, Development and Optimization of Solid Lipid Nanoparticle Containing Fluconazole and Its Anti-Fungal Activity," *Int. J. Innov. Sci. Eng. Manag.*, vol. 5, no. 1, 2026, doi: 10.69968/ijsem.2026v5i1134-45.
- [5] E. TawsifEfaz *et al.*, "A review of primary technologies of thin-film solar cells," *Eng. Res. Express*, vol. 3, 2021.
- [6] Y. E. Ahmed, M. R. Maghami, J. Pasupuleti, S. H. Danook, and F. B. Ismail, "Overview of Recent Solar Photovoltaic Cooling System Approach," *Technologies*, vol. 12, no. 171, 2024.
- [7] S. Gorjian and H. Ebadi, "Photovoltaic Solar Energy Conversion," *Elsevier*, 2020, doi: 10.1016/B978-0-12-819610-6.00001-6.
- [8] H. A. Hasan *et al.*, "Experimental Evaluation of the Thermoelectrical Performance of Photovoltaic-Thermal Systems with a Water-Cooled Heat Sink," *Sustainability*, vol. 14, 2022.
- [9] L. K. Alexis, K. L. Stephane, P. M. J. Pierre, M. K. Fabrice, and T. J. Kewir, "Development and Experimental Evaluation of a New Photovoltaic-thermal Air Collector to Optimise the Performance of PV Solar Modules," *Int. J. Sustain. Green Energy*, vol. 15, no. 1, pp. 31–44, 2026.
- [10] H. Choi and K.-H. Choi, "Performance Evaluation of PVT Air Collector Coupled with a Triangular Block in Actual Climate Conditions in Korea,"

- Energies*, vol. 15, 2022.
- [11] C. Wang, F. Guo, H. Liu, and G. Wang, "A Comprehensive Review of Research Works on Cooling Methods for Solar Photovoltaic Panels," *Energies*, vol. 18, no. 4305, pp. 1–43, 2025.
- [12] F. Rubbi, L. Das, K. Habib, N. Aslfattahi, R. Saidur, and M. T. Rahman, "State-of-the-art review on water-based nanofluids for low temperature solar thermal collector application," *Sol. Energy Mater. Sol. Cells*, vol. 230, 2021, doi: 10.1016/j.solmat.2021.111220.
- [13] A. Sarojwal and A. Garg, "Enhancing Solar PV Array Output and Efficiency through IoT- Based Modern Techniques," *Int. J. Innov. Sci. Eng. Manag.*, vol. 3, no. 2, pp. 214–222, 2024, doi: 10.69968/ijisem.2024v3si2.
- [14] M. Taguchi, A. Suzuki, N. Ueoka, and T. Oku, "Effects of poly(methyl methacrylate) addition to perovskite photovoltaic devices," *AIP Conf. Proc.*, vol. 2067, 2019, doi: 10.1063/1.5089451.
- [15] M. Mustapha, A. Fudholi, C. H. Yen, M. H. Ruslan, and K. Sopian, "Review on Energy and Exergy Analysis of Air and Water Based Photovoltaic Thermal (PVT) Collector," *Int. J. Power Electron. Drive Syst.*, vol. 9, no. 3, 2018, doi: 10.11591/ijpeds.v9.i3.pp1367-1373.
- [16] I. O. Harmailil, S. M. Sultan, C. P. Tso, A. Fudholi, M. Mohammad, and A. Ibrahim, "A review on recent photovoltaic module cooling techniques: Types and assessment methods," *Results Eng.*, vol. 22, 2024, doi: 10.1016/j.rineng.2024.102225.
- [17] I. O. Harmailil, S. M. Sultan, C. P. Tso, A. Fudholi, M. Mohammad, and A. Ibrahim, "The State of the Art of Photovoltaic Module Cooling Techniques and Performance Assessment Methods," *Symmetry (Basel)*, vol. 16, no. 412, 2024.
- [18] M. Alktrane and P. Bencs, "Experimental comparative study on using different cooling techniques with photovoltaic modules," *J. Therm. Anal. Calorim.*, vol. 148, pp. 3805–3817, 2023, doi: 10.1007/s10973-022-11940-1.
- [19] A. Samsudin *et al.*, "Recent advances in photovoltaic thermal collectors (PVT): from conventional designs to high insulation glazing and semi-transparent PVT for building applications," *J. Build. Eng.*, vol. 116, 2025, doi: 10.1016/j.job.2025.114500.
- [20] W. H. Saleh, A. A. Jadallah, and A. L. Shurajji, "A-Review for the Cooling Techniques of PV/T Solar Air Collectors," *Eng. Technol. J.*, vol. 40, no. 1, pp. 129–136, 2022.
- [21] M. M. Farag, A. Hamid, M. N. AlMallahi, and M. Elgendi, "Towards highly efficient solar photovoltaic thermal cooling by waste heat utilization: A review," *Energy Convers. Manag. X*, vol. 23, 2024, doi: 10.1016/j.ecmx.2024.100671.
- [22] M. Ahmed, M. F. Baig, E. E. M. Noor, and M. A. Musa, "Optimizing photovoltaic-thermal systems: a comprehensive indoor experimental investigation," *Cogent Eng.*, vol. 12, no. 1, p., 2025, doi: 10.1080/23311916.2025.2524447.
- [23] F. Ghaith, T. Siddiqui, and M. Nour, "Design of Solar-Powered Cooling Systems Using Concentrating Photovoltaic/Thermal Systems for Residential Applications," *Energies*, vol. 17, no. 4558, 2024.
- [24] S. S. H. Hajjaj, A. A. M. T. H. S. Aqeel, F. S. Shahar, and A. U. M. Shah, "Review of Recent Efforts in Cooling Photovoltaic Panels (PVs) for Enhanced Performance and Better Impact on the Environment," *Nanomaterials*, vol. 12, no. 1664, pp. 1–18, 2022.
- [25] M. R. Sharaby, M. R. Sharaby, M. M. Younes, F. S. A. Taleb, and F. B. Baz, "The impact of hybrid nanofluid cooling on photovoltaic/thermal system performance: a 3E analysis approach," *J. Therm. Anal. Calorim.*, vol. 150, pp. 19575–19589, 2025, doi: 10.1007/s10973-025-14889-z.
- [26] A. Parthiban, K. S. Reddy, B. Pesala, and T. K. Mallick, "Effects of operational and environmental parameters on the performance of a solar photovoltaic-thermal collector," *Energy Convers. Manag.*, vol. 205, 2020.